We are IntechOpen, the world's leading publisher of Open Access books Built by scientists, for scientists

4,800
Open access books available

122,000
International authors and editors

135M
Downloads

Our authors are among the

154
Countries delivered to

TOP 1%
most cited scientists

12.2%
Contributors from top 500 universities

WEB OF SCIENCE™

Selection of our books indexed in the Book Citation Index in Web of Science™ Core Collection (BKCI)

Interested in publishing with us?
Contact book.department@intechopen.com

Numbers displayed above are based on latest data collected.
For more information visit www.intechopen.com

19

Numerical Modeling of Wet Steam Flow in Steam Turbine Channel

Hasril Hasini, Mohd. Zamri Yusoff and Norhazwani Abd. Malek
Centre for Advanced Computational Engineering, College of Engineering, University Tenaga Nasional, Malaysia

1. Introduction

In power station practice, work is extracted from expanding steam in three stages namely High Pressure(HP), Intermediate Pressure(IP) and Low Pressure(LP) turbines. During the expansion process in the LP turbine, the steam cools down and at some stages, it nucleates to become a two-phase mixture. It is well-acknowledged in the literature that the nucleating and wet stages in steam turbines are less efficient compared to those running with superheated steam. With the advent of water-cooled nuclear reactor, the problem becomes more prominent due to the fact that in water-cooled nuclear reactor, the steam generated is in saturated condition. This steam is then supplied to the HP steam turbine which therefore has also to operate on wet steam. One of the tangible problems associated with wetness is erosion of blading. The newly nucleated droplets are generally too small to cause erosion damage but some of the droplets are collected by the stator and rotor blades to form films and rivulets on the blade and casing walls. On reaching the trailing edges or the tips of the blades, the liquid streams are re-entrained into the flow in the form of coarse droplets. It is these larger droplets that cause the erosion damage and braking loss in steam turbine. However, the formation and behaviour of the droplets have other important thermodynamic and aerodynamic consequences that lower the performance of the wet stages of steam turbines.

Interest in wet steam research was sparked by the need for efficient steam turbines used in power generation. The subject has become increasingly important in current decades with the steep increase in fuel cost. The importance of steam turbine in society is obvious considering that most of the world's power generation takes place using steam-driven turbines. Even though the importance of these machines is obvious, very little attention is given by researchers to understanding the flow behaviour inside steam turbines in comparison with other prime movers. Considerable progress has been made in the investigation of flow in gas turbines because of their applications in the aeronautical field. The findings from gas turbine research are applicable to the dry stage in steam turbine only. However, attention must also be paid to the wet stages as a significant proportion of the output is generated by them. In recent years, work in wet steam research has gained interest with the advent of high performance computing machines and measurement devices. Most of the works aim to accurately model the droplet formation using different calculation

method such as quadrature method of moments (Gerber & Mousavi, 2007). Attempt was also made to use commercial CFD package to calculate the three dimensional steam properties (Dykas et al., 2007, Nikkhahi et al. 2009, Wroblewski et al., 2009).

2. Literature review

2.1 Early Investigations

Among the pioneers in the investigation of thermodynamic condensation was (Aitken, 1880), who in his experiments in 1880 observed that any dust or salt particles present in the expansion of saturated air will act as centres for condensation. A similar investigation was also carried out by (Von Helmholtz, 1886) but it was (Wilson, 1897) who made a detailed study of spontaneous condensation where it was found that in the absence of ions or foreign nuclei during the expansion of saturated air, condensation was delayed. The formulation of the ratio of vapour pressure, P to the saturation pressure corresponding to local vapour temperature $P_s(T_G)$ was later formulated and called supersaturation ratio, S. This parameter is used as a measure of supersaturation and is given by:

$$S = \frac{P}{P_S(T_G)} \tag{1}$$

Supersaturation ratio, S measures the departure of fluid from thermodynamic equilibrium. Subsequently, (Henderson, 1913) reported that the discharge of steam in nozzles, expanding in the wet region in Mollier chart was approximately 5% greater than the value that would be expected from equilibrium calculations. Following this observation, (Stodola, 1915) published his own results of nozzle expansions. A thorough discussion of supersaturation effects in nozzles was first given by (Callender, 1915). His discussion includes a prediction of droplet size based on the Kelvin–Helmholtz equation. Subsequently, by assuming that condensation will always produce droplets of similar size, (Martin, 1918) calculated the limiting supersaturation at other pressures and plotted them on the Mollier chart. This limiting supersaturation line is called Wilson line. For the next 10 years, much work on spontaneous condensation was carried out by Stodola and most of his work is summarized in his book, (Stodola, 1927).

2.2 Nucleation theory

The development of nucleation theory started almost at the same time as the study of condensation but significant results were obtained only after 10 years. Among the earlier investigators on limiting supersaturation were (Yellot, 1934), Yellot & Holland, 1937; Rettaliata, 1938). In their works, attempts were made to define the position of Wilson line more precisely. It was found that the limiting supersaturation was dependent on the nozzle shape and experimental condition and they suggested the replacement of the Wilson line by Wilson zone. Following his work, (Binnie & Woods, 1938) and (Binnie & Green, 1943) performed further accurate measurement of axial pressure distribution in nucleating flows in convergent-divergent nozzles.

The nucleation theory was first combined with the gas dynamics equations by (Oswatitsch, 1942). He applied the treatment to condensing flows of water vapour in nozzles both as pure vapour and part of atmospheric air and reported good agreement with experimental observations. In parallel with the investigations mention, the development of steam turbines

was progressing with remarkable speed and the problems associated with the presence of liquid were being experienced. One of the particular serious consequences resulting from the presence of liquid in steam turbines is blade erosion. However, with the introduction of reheat cycles after the Second World War, the problem was temporarily alleviated. Following new developments and designs of larger steam turbine, the steam velocity could reach much higher values. This led to considerable impact velocities which brought renewed interest in wetness problems. Among the many researchers who have reported their investigations into the field are (Gyarmathy, 1962, Pouring, 1965, Hill, 1966, Puzyrewski, 1969, Wegener, 1969, Campbell & Bakhtar, 1970, Barschdorff, 1970, Filippov & Povarov, 1980). In addition to these investigations, a number of studies aimed at measuring the size of droplets formed by spontaneous nucleation were reported by (Gyarmathy & Meyer, 1965, Krol, 1971, Deich et al., 1972). The measurements have provided further data for comparison with the theoretical solutions.

2.3 Condensation in nozzle

An expansion of steam from superheated to wet condition in a typical convergent-divergent nozzle is illustrated in Fig. 1. The process can be also illustrated on an $h - s$ diagram as shown in Fig. 2. Steam enters the nozzle as dry superheated vapour at point (1) and during its passage through the nozzle, it expands to the sonic condition represented by point (2). At point (3) in Fig. 2, the saturation line is crossed which may occur before or after the throat and droplet embryos begin to form and grow in the vapour. The nucleation rates associated with these early embryos are so low that the steam continues to expand as a dry single-phase vapour in a metastable, supercooled or supersaturated state. Depending on the local conditions and the rate of expansion, the nucleation rate increases dramatically and reaches

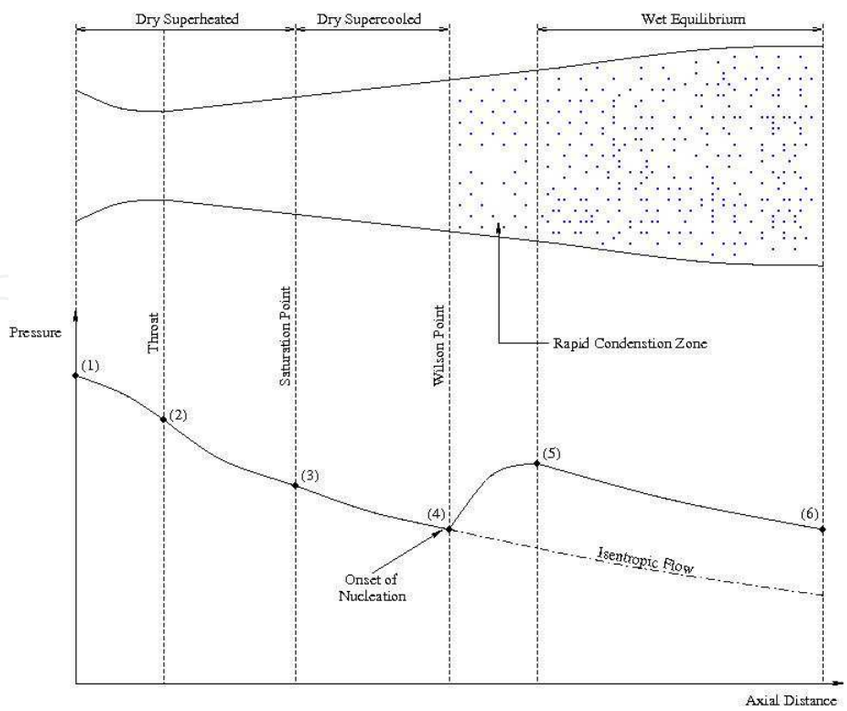

Fig. 1. Axial pressure distribution in nozzle with spontaneous condensation.

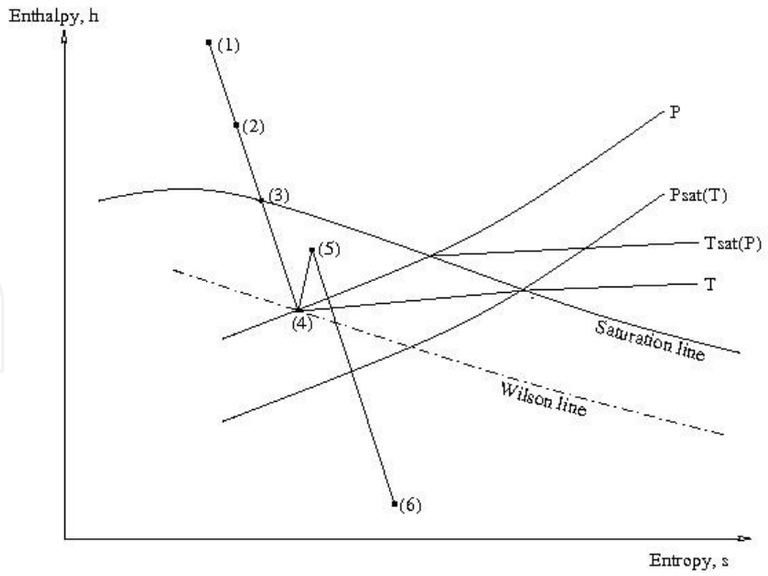

Fig. 2. State line for expanding steam with spontaneous condensation.

its maximum at point (4). This area is termed nucleating zone and is terminated by the Wilson point, which is the point of maximum supercooling and is defined as:

$$\Delta T = T_S(P) - T_G \tag{2}$$

Downstream of this point, nucleation ceases effectively and the number of droplets in the flow remains constant. The nuclei grow rapidly between points (4) and (5) and restore the system to thermodynamic equilibrium. Further expansion of the flow between points (5) and (6) takes place close to equilibrium conditions.

3. Governing equations for two-phase wet steam flow

Assuming no inter-phase slip, the volume occupied by the liquid to be very small and that the vapour phase behaves as a perfect gas, the fundamental equations of motion for steady 1-D flow of a condensing vapour over an incremental distance *dx* along duct axis shown in Fig. 3 can be written as:

Continuity:

$$m = m_G + m_L = constant \tag{3}$$

And

$$m_G = \rho_G A u \tag{4}$$

where m is the mass flow rate, ρ is the density, A is the area and u is the velocity. The suffixes G and L denote the vapour and liquid phase respectively. Using the definition of Eq. (4), Eq. (3) can be written in differential form as:

$$\frac{d\rho_G}{\rho_G} + \frac{dA}{A} + \frac{du}{u} + \frac{dm_L}{m - m_L} = 0 \tag{5}$$

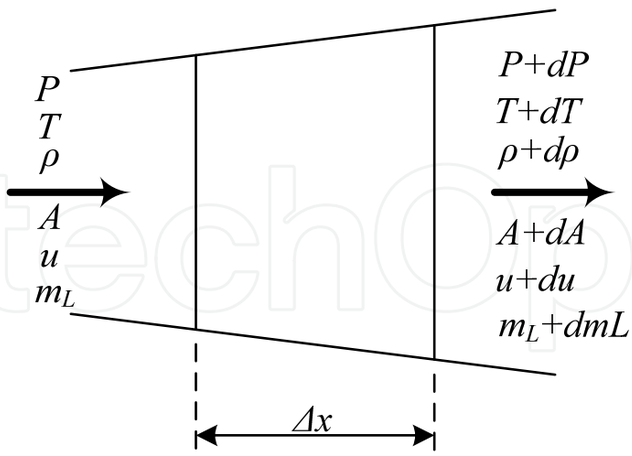

Fig. 3. Control volume for 1D flow analysis.

Momentum:

$$\frac{dP}{P} + \frac{\rho_G\, u^2}{\rho}\,\frac{f\, dx}{2\, d_e} + \frac{\rho_G\, u^2}{(1-\omega)P}\,\frac{du}{u} = 0 \tag{6}$$

Where P is the pressure, f is the friction factor, ω is the wetness fraction and d_e is the hydraulic mean diameter for the duct section.

Energy:

$$\frac{u^2}{c_P\, T_G}\,\frac{du}{u} + \frac{dT_G}{T_G} + \frac{d(\ell\, m_L)}{c_P\, T_G\, m} = 0 \tag{7}$$

Where c_P is the specific heat at constant pressure, T is the temperature and ℓ denotes the energy given up by unit mass of vapour on condensing.

Equation of state:

$$\frac{dP}{P} - \frac{d\rho_G}{\rho_G} - \frac{dT_G}{T_G} = 0 \tag{8}$$

Condensing flow of steam may be regarded as a special case of the flow of a compressible fluid in a duct with friction and heat addition in which heat added to the flow is the result of the phase change, which also affects the mass flow rate. In the analysis of one-dimensional condensing flow, steam is assumed to consist of liquid droplets of specified sizes and uniformly distributed in parent vapour which fills the space between them. The treatment combines the droplet formation and growth equations with one-dimensional gas dynamics equation. The relationship between the vapour pressures over a curved surface to its radius of curvature at low pressure is given by the Kelvin-Helmholtz equation. The equation is modified to include higher virial coefficients and is given by:

$$r^* = \frac{2\sigma}{\rho_L\, R\, T_G \ln\left\{{}^{p}/_{p_s\,(T_G)} + 2B\,[\rho - \rho_s]\right\}} \tag{9}$$

where r^* is the critical droplet radius, σ is the surface tension of liquid droplet, R is the gas constant, $p_s(T_G)$ is the saturation pressure corresponding to local vapour temperature T_G and B is the virial coefficient. For given vapour conditions, droplets with radius r^* will be in unstable equilibrium with the vapour condition. For equilibrium, larger droplets need a lower supersaturation and will grow. On the other hand, smaller droplets will find the surrounding supercooling state insufficient and therefore tend to evaporate. In order to condense, the molecules must form droplet of radius r^* which is against their natural tendency. The only route to the formation of super-critical droplets is through collision within the body of the vapour. From eq. (7), it can be seen that the critical radius is inversely proportional to the supersaturation (p/p_s) and therefore, the lower the supersaturation, the larger the size of critical droplets and the smaller the chance that new droplet embryo will be formed.

Original investigation of the rate of formation of critical clusters within the supercooled vapour was carried out by (Volmer & Weber, 1996, Farkas, 1927, Becker & Doring, 1935, Frenkel, 1946, Zeldovich, 1942). This was later refined, modified and reviewed by numerous investigators. The expression for the nucleation rate as the number of droplets formed per unit volume and time as given by the classical nucleation theory is:

$$J = q\left(\frac{2\sigma}{\pi m^3}\right)^{1/2} \frac{{\rho_G}^2}{\rho_L} exp\left[-\frac{4\pi r^* \sigma}{3\, k\, T_G}\right] \tag{10}$$

where J is the nucleation rate, k is the Boltzmann's constant and q is the condensation coefficient, which is defined as the fraction of molecular collisions which results in condensation. Substituting for critical radius, r^* in terms of the supersaturation ratio, it will be seen that very small changes in the supersaturation of the fluid can influence the nucleation rate drastically.

Condensation occurs by the nucleation of new droplets and the growth of any existing droplets within specified incremental step. The incremental mass of liquid formed, dm_L can be determined by using the nucleation and droplet growth equations. The equation for nucleation rate is derived from classical nucleation theory. Once the mass of liquid over an incremental step is known and regarding the terms $\frac{fdx}{2d_e}, \frac{dA}{A}$ and dm_L as independent variables, Eqns. 5-8 can be solved for four unknowns, $\frac{du}{u}, \frac{dT_G}{T_G}, \frac{dP}{P}$ and $\frac{d\rho_G}{\rho_G}$. The resulting expression can be integrated using fourth order Runge-kutta technique to yield the changes in the flow properties over the step. But to increase the accuracy of the coupling between the main flow equation and the equations describing droplet behavior, the calculation is carried out in the following steps:

1. The droplet growth equations are integrated at constant inlet pressure, P_{in} and temperature, $T_{G,in}$ to the element Δx to obtain the first approximation to the values of m_L and dm_L.
2. The values of m_L *and* dm_L found in Eq. 3 are inserted into the flow equations which are then integrated to give a first approximation for the exit consition, P_{out} and $T_{G,out}$.
3. The droplet growth equation are integrated for a second time over Δx, assuming constant vapour condition, P_{out} and $T_{G,out}$ and new values of m_L and dm_L are calculated.

4. The values of m_L and dm_L found from Eq. 3 and Eq. 5 are averaged and assumed to represent the variables over incremental step, Δx.
5. Using the average values of m_L and dm_L found in Eq. 6, the flow equations are integrated to obtain the final values of P_{out} and $T_{G,out}$.
6. To ensure that all properties are compatible, the droplet temperature at exit is adjusted so that it correspond to the mean droplet radius.

Then starting at inlet to the nozzle, the flow equations are integrated step by step until the end of nozzle is reached.

In this investigation, upon completion of the nucleation phase, the properties of fluids are calculated based on the two methods. The first method is carried out by combining all droplet groups into a single population and their properties are averaged when there is no new droplet embyo forms in the subsequent step length. This is called the "Average" method. The other method of calculation is when every single droplet groups and their properties are retained even after the completion of nucleation phase. This is called the "Non-Averaged" method. The droplet radius calculation using this method is based on r.m.s. values for each droplet group. In theory, this method should results in more accurate solution but it requires an extremely huge processing power to complete the whole calculation.

4. Results, analysis and discussion

4.1 Calculation on dry, steady flow

In order to test for the accuracy of the numerical code, the model was applied to a few test cases at dry condition in a convergent-divergent nozzle. Three cases were calculated namely the subsonic-supersonic flow, purely subsonic flow and the flow involving shock. In this test, the inlet temperature and total pressure for all cases are set to 421.3K and 72,700 Pa respectively while the back pressure is varied according to the desired cases. For purely subsonic case, the back pressure is set to 68,000 Pa (giving a pressure ratio of 1.069) while for the supersonic flow, linear interpolation is employed for the determination of the back pressure. On the other hand, the back pressure for the shock case is set to 60,400 Pa.

Fig. 4 illustrates the general Mach number distribution along x direction for all cases. The numerical results are compared with the exact solutions which are given by solid lines close to each case respectively. It can be clearly seen that all numerical results show a slight deviation from the exact solutions except for the supersonic case where both numerical and exact solutions agrees very well with each other. For the pure subsonic flow case, the Mach number increases with distance until it reaches a peak value of 0.57 at the throat. Downstream of the throat, the Mach number decreases in the divergent section due to the decrease in the flow velocity. Comparison with the exact solution shows a slightly higher value and this could be attributed to the numerical error presented in the model. For the subsonic-supersonic case, the Mach number increases along the nozzle. The numerical solution for this case shows good agreement with the exact solution. The Mach number increases starting from the nozzle inlet to the nozzle exit. In order to emulate the shock case, the exit pressure is reduced slightly below the pressure imposed on the subsonic case. A

normal shock-wave was found slightly downstream of the throat in the divergent section of the nozzle. The flow is supersonic upstream the normal shock-wave, whereas it becomes subsonic downstream the normal shock-wave.

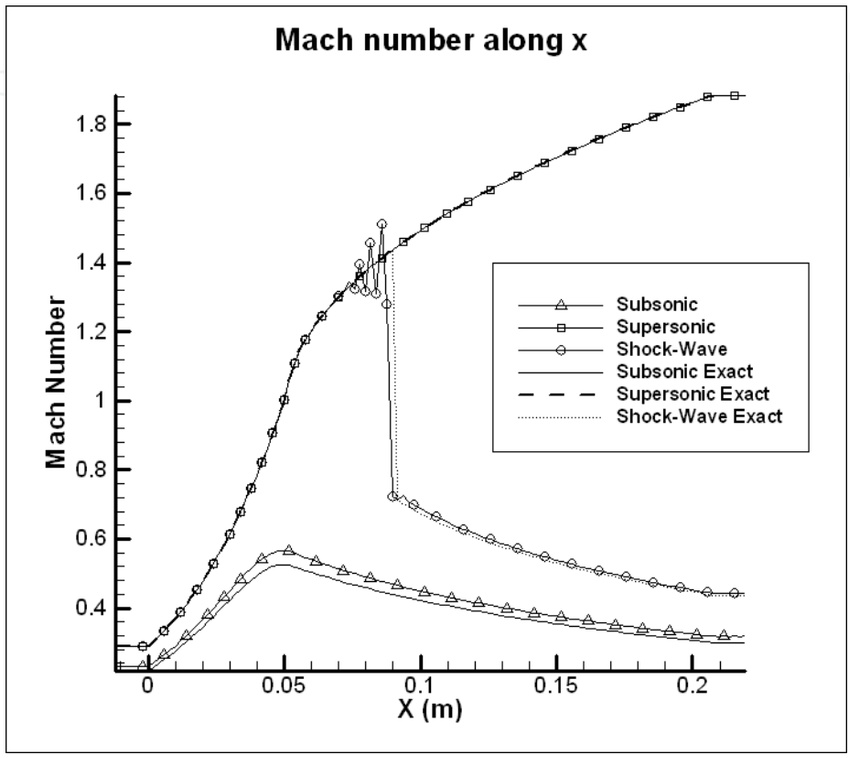

Fig. 4. Comparisons of Mach number using numerical solution and exact solution (for dry case).

In addition to the Mach number, the pressure variation along the distance is also investigated and this is illustrated in Fig. 5. For the subsonic case, the pressure decreases along the nozzle length due to the reduction in flow area (where the velocity increases). Minimum pressure is calculated at the throat and the pressure increases again downstream of the throat due to the increase in flow area. For the supersonic case however, the pressure decreases starting from the nozzle inlet towards the nozzle exit. Downstream of the throat where choking occurs, the velocity of the fluid further increases thus reducing the pressure further. On the other hand, for the shock case, the pressure distribution is similar to the supersonic case except for a location downstream of the throat where sudden jump in pressure is observed indicating shock. It is also worth mentioned that prior to the shock, obvious oscillations can be seen due to the adoption of the central discretization scheme in the calculation which is highly unstable. Although artificial viscosity has been added to the equations, it is believed that the value is either too small or too large to improve the stability of the solutions. Thus further investigation is needed to eliminate or at least minimize the oscillation. Downstream the shock position, the pressure further increases towards the nozzle exit.

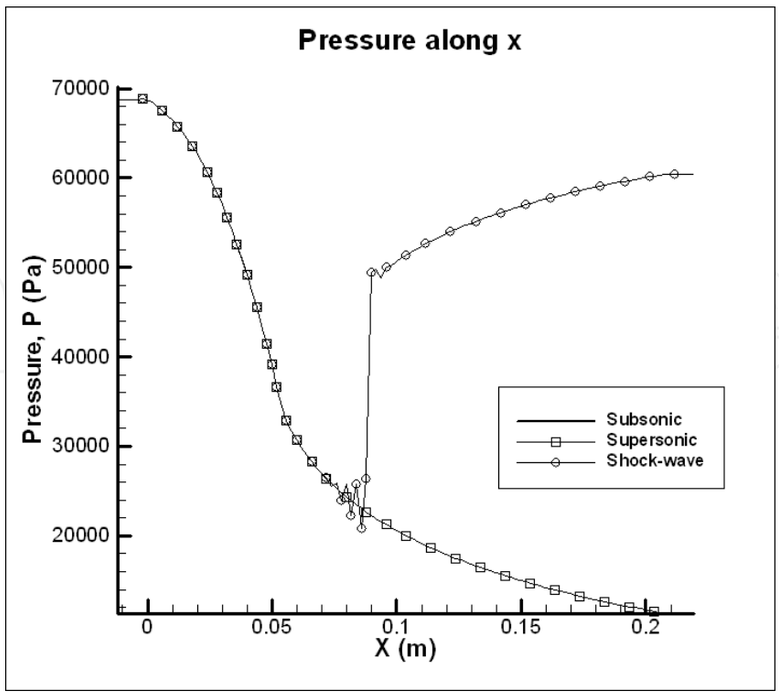

Fig. 5. Pressure variations using numerical solution and exact solution (dry case).

4.2 Steady flow wet steam simulation

Based on the prediction made on dry condition on a few test cases, it has been demonstrated that the numerical scheme is able to calculate the compressible flow properties with good accuracy. The next step involves the calculation of two-phase flow properties using similar scheme but with the addition of the wetness treatment. The numerical scheme was applied to three cases involving nucleating steam flows in one-dimensional nozzles. These nozzles are those of (Binnie and Wood, 1938), (Krol, 1971) and (Skillings, 1987). The exact boundary conditions imposed for these cases are summarized in Tab. 1. For all tests, the flow with condensation takes place.

Nozzle		P_0 (Pa)	T_0 (K)	$T_{sat}(P)$ (K)
Binnie and Wood (1938)		143,980	391.87	383.28
Krol (1971)	Case 1	221,000	423.00	396.60
	Case2	294,000	453.00	405.96
Skillings (1987)	Case 1	32,510	357.20	344.60
	Case 2	35,440	349.00	346.13

Table 1. Boundary conditions for different test cases.

In the one dimensional calculation, the number of node used in all cases is 125. In addition to the comparison made with the experimental data (where available), the 2D results of the same method are also plotted for comparisons. The 2D calculation was carried out in a few nozzle configurations namely (Binnie & Wood 1938), (Kroll, 1971) and (Skilling, 1987). For each of these nozzles, structured mesh with consistent size of 125 × 15 is adopted and is illustrated in Fig. 6.

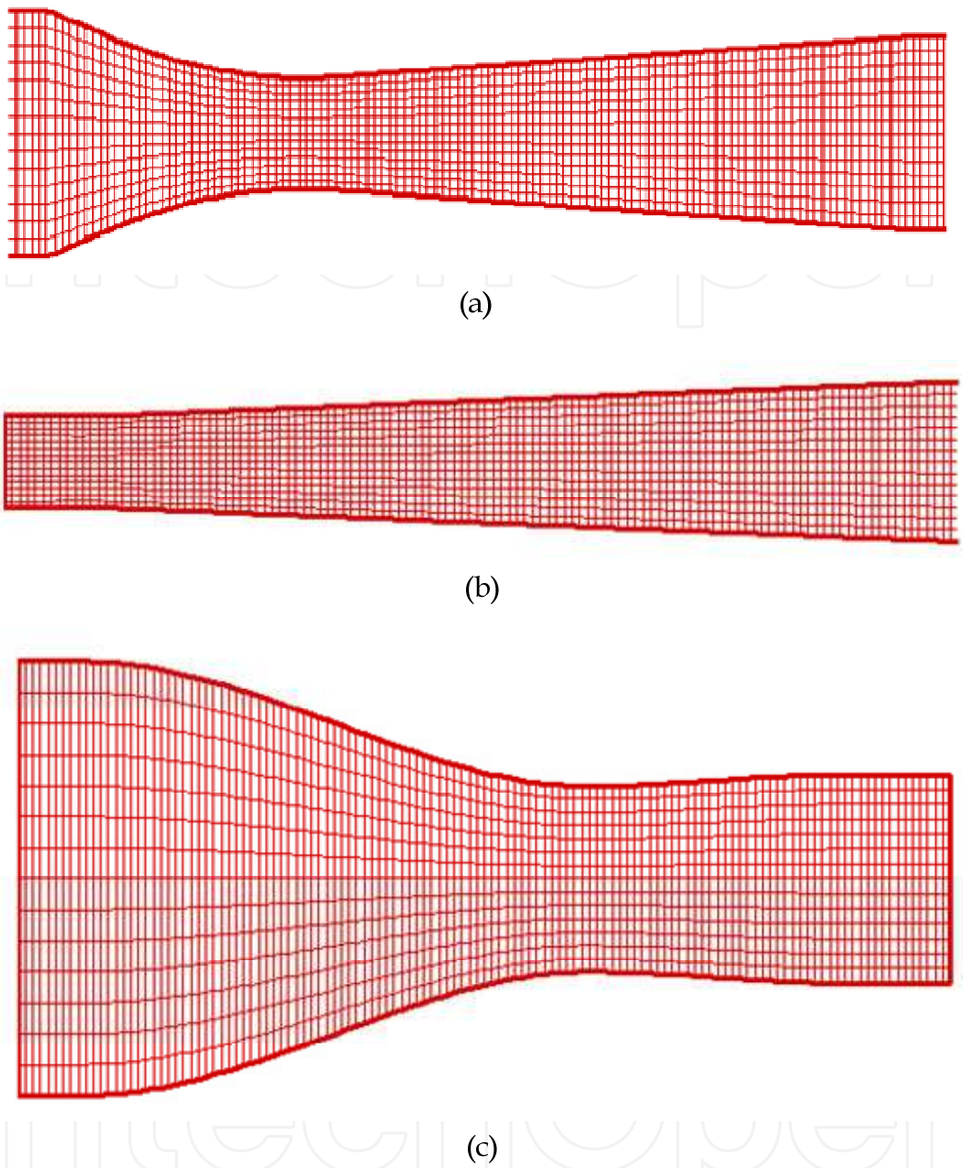

(a)

(b)

(c)

Fig. 6. 2D mesh for different nozzles (a) Binnie & Wood; (b) Kroll (c) Skilling.

Fig. 7 shows the pressure ratio distribution along nozzle length based on (Binnie &Wood, 1938). The general distribution on the pressure shows a decreasing trend due to the increase in velocity. The onset of condensation can also be observed by the sudden jump in pressure when condensation occurs and is typical for wet supersonic expansions. This is due to the release of latent heat at supersonic conditions which tends to retard the supersonic flow. The trend continues to decrease downstream of the throat towards the nozzle exit. The distributions of pressure along the nozzle predicted are in good agreement with experimental data.

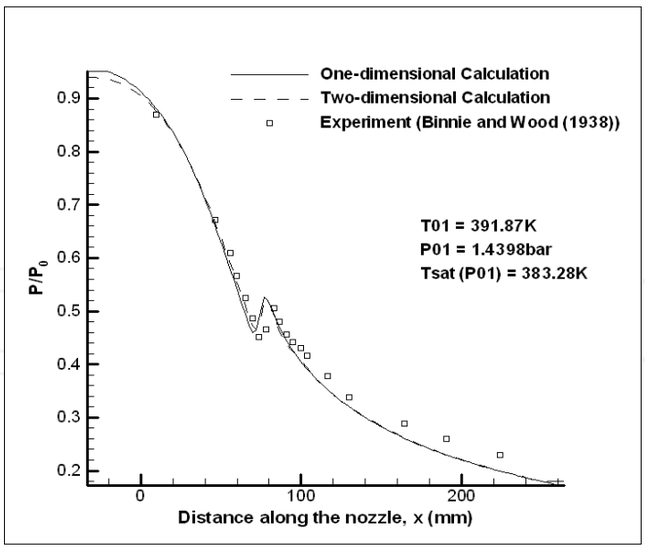

Fig. 7. Comparison of pressure ratio along Binnie and Wood nozzle.

Fig. 8(a) and 8(b) shows the pressure distribution along Krol nozzle for Case 1 and Case 2 respectively. The calculated pressure distribution for 1D and 2D cases show an excellent agreement for Case 1. However, experimental validation could not be made for this case due to the absent of experimental data. In order to increase confidence in the current scheme however, the model was validated with Case 2 where detail measurement was present. The comparison between the 1D and 2D calculation against experimental data is illustrated in Fig. 8(b). Despite the absent of data upstream of the nozzle throat, reasonable agreement was achieved downstream of the throat.

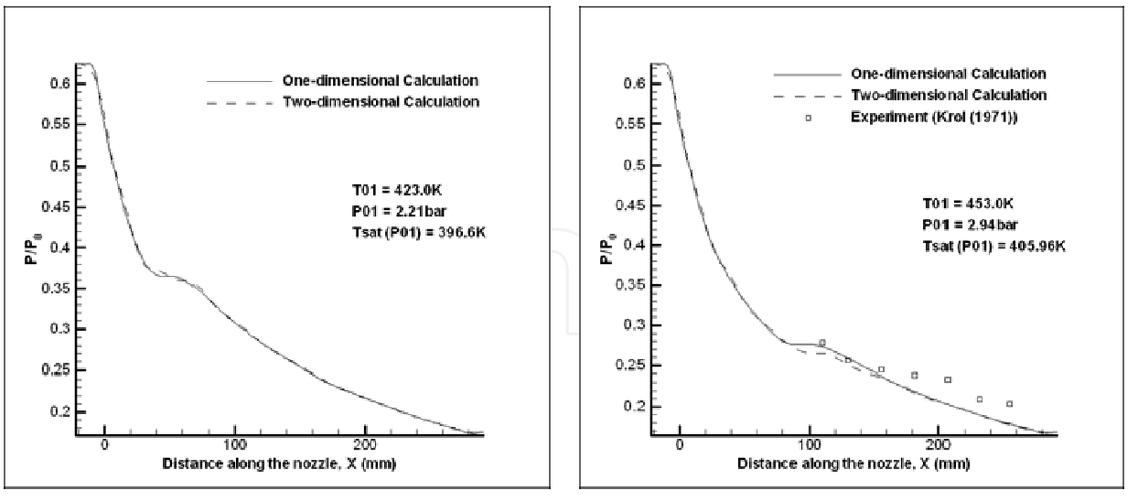

(a) (b)

Fig. 8. Comparison of pressure distribution along Krol nozzle for (a) Case 1 (b) Case 2.

In addition to the Binnie & Wood and Krol nozzles, the mathematical model is also tested on Skilling nozzle (Skilling, 1987) at two different boundary conditions (Case 1 and 2). This is shown in Figs. 9(a) and 9(b) respectively. The general pressure distribution shows a

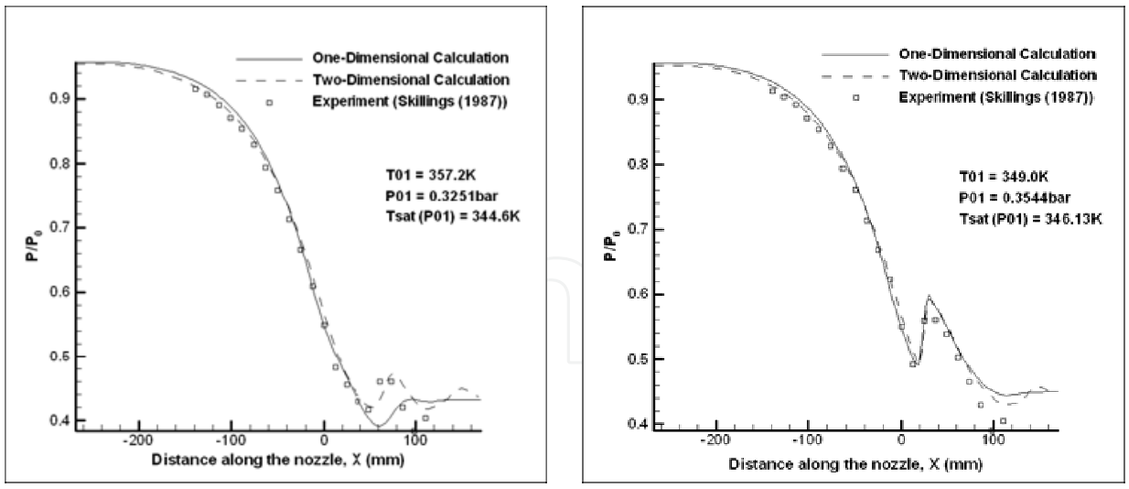

(a) (b)

Fig. 9. Comparison of pressure distribution along Skilling nozzle for (a) Case 1 (b) Case 2.

decreasing trend when the flow was expected to increase in reduced cross sectional area. Comparison with the experimental result reveals good agreement. In addition, the onset of condensation was predicted correctly for both cases. From this calculation, it is evident that the location where condensation begins is highly influenced by the inlet temperature imposed on the inlet boundary.

To quantitatively validate the calculation model, comparison is also made based on the droplet size and its distribution along the duct. Fig. 10 shows the distributions of droplet radius for 1D and 2D calculations in Binnie & Wood nozzle. It can be seen that the droplet starts to form slightly downstream of the throat, grows rapidly if the surrounding parent vapour permits, and continue to grow towards the exit. It is these droplets that contribute to the wetness inside turbine channel. The droplet size information for the 2D case was taken at stream centre with the assumption of constant fluid properties along the *y*-direction. It is believed that the actual properties vary at least slightly in this direction, thus contributing to the slight deviation as compared to the 1D result. The 2D calculation shows slightly higher droplet radius after rapid growth downstream of the throat and this can be attributed to the cumulative contribution of different sets of droplet groups from the region in *y*-direction which was not accounted for the calculation.

Fig. 11(a) and 11(b) show the comparison made on the calculated droplet radius with experimental data on Krol nozzle (Krol, 1971) for Case 1 and Case 2 respectively. The general trend on the size distribution is almost identical for all nozzles, i.e. droplet grows rapidly once it is formed and continues to grow at a slower rate towards the nozzle exit. For Case 1, reasonable agreement was achieved for the 2D calculation. However, the 1D model was unable to predict the droplet size accurately despite showing similar growth profile. This discrepancy could be attributed to the two-dimensional effect in nozzle flow where the property variation in *y*-direction is important and needs to be taken into account in the calculation. In this case, the 1D calculation has over-predict the droplet radius due to the faster expansion rate for Kroll nozzle as compared to the Binnie & Wood nozzle. For Case 2, similar trend was shown at which better prediction was made by the 2D model as compared

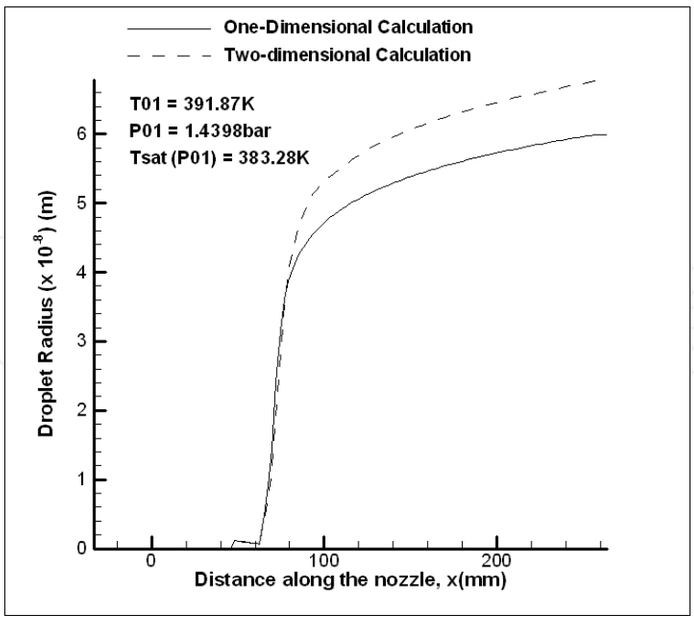

Fig. 10. Comparison of droplet size along Binnie & Wood nozzle (Binnie and Wood, 1938).

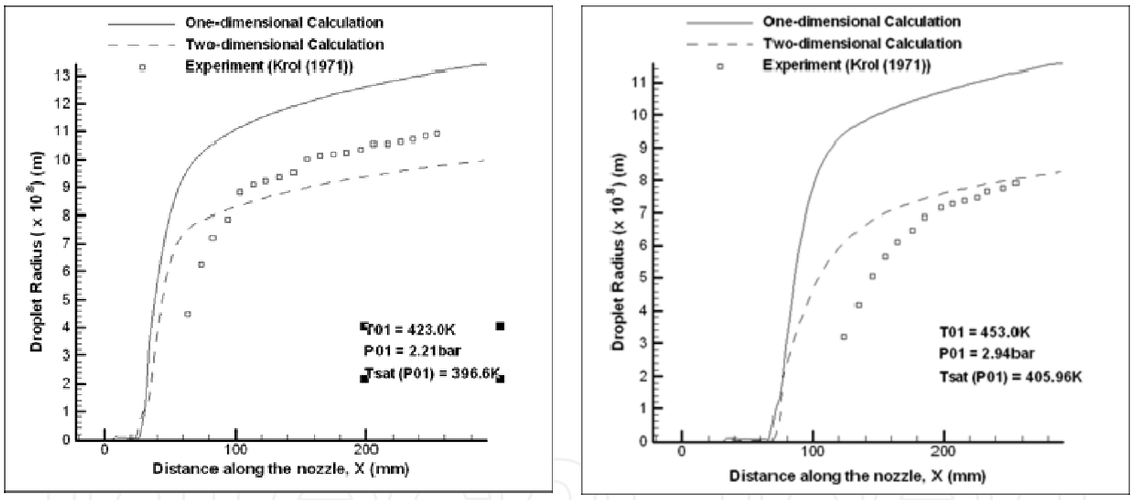

(a) (b)

Fig. 11. Comparison of droplet size distribution in Krol nozzle for (a) Case 1 (b) Case 2.

to the one dimensional model. Based on these figures, it is also interesting to note that the temperature imposed at the inlet boundary has significant effect in delaying the onset of condensation. This has been demonstrated by Case 1 which inlet total temperature is lower than Case 2, thus results in the faster droplet formation and growth.

In addition to Binnie & Wood and Krol nozzles, further test is also carried out to investigate the ability of the model to calculate the droplet size distribution inside the channel. The third test case was done by adopting the Skilling nozzle where droplet size measurement was available. Fig. 12(a) and 12(b) illustrate the comparison on the droplet size along the nozzle for Case 1 and Case 2 respectively. In Case 1, the inlet total temperature was set

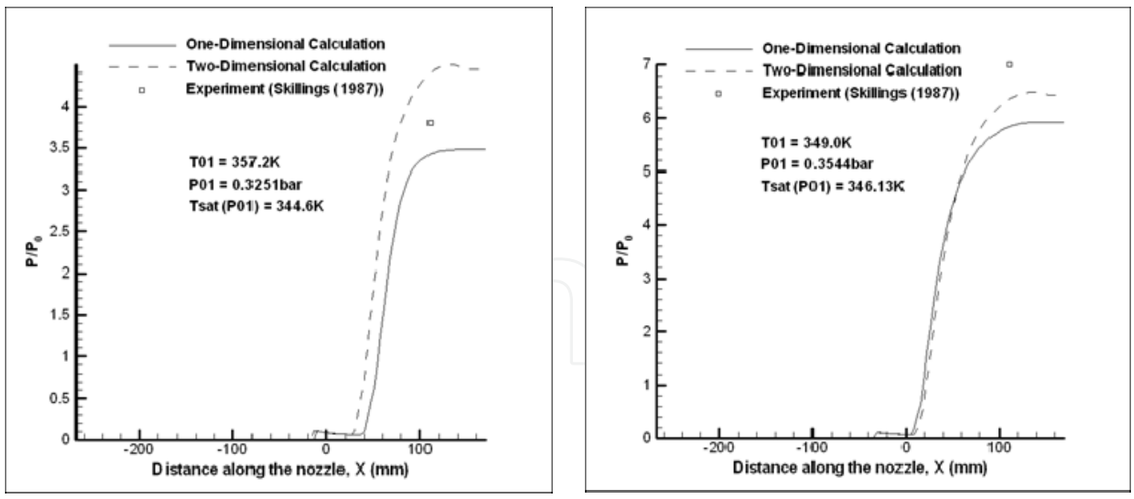

(a) (b)

Fig. 12. Comparison of droplet size distribution along Skilling nozzle for (a) Case 1 (b) Case 2.

higher than Case 2 with the value of 357.2 K, thus there is a slight delay in the formation of droplet embryo. In this case, the droplet starts to form slightly downstream of the throat region, undergoes rapid growth and terminates at nozzle exit. Based on Fig. 12(a), the 1D model has under-predict the droplet size, while the 2D model has over-predict the size. For Case 2, the inlet total temperature is set lower (349 K), thus the formation of droplet embryo occurs earlier somewhere in the throat region and grows rapidly once the saturation condition is met. Reasonable accuracy was achieved both for 1D and 2D cases. In this case, both 1D and 2D calculations have under-predict the droplet size. Similar to Case 1, only one experimental reading was available thus qualitative comparison on droplet size distribution along the nozzle was not possible. It is difficult to quantitatively compare the distribution of droplet size along the nozzle since only one reading was made available (Skilling, 1987) for each case.

4.3 Unsteady supercritical heat addition

In wet steam flows, condensation in a nozzle usually occurs in the divergent section just downstream of the throat with the consequence of the considerable release of latent heat, Q, to the flow. In addition, this phenomenon has the effect of moving the flow Mach number to unity. This is due to the addition of heat to the supersonic flow, which causes it to decelerate. The effect produced when Mach number equals to unity was described as "thermal choking" (Pouring, 1965) and when this happens, the flow can no longer sustain the additional heat and becomes unstable. The excess quantity of this additional heat is termed supercritical heat addition and has caused the flow to be unstable. This phenomenon commonly occurs in high speed condensing flow has been studied in detail by (Barschdoff, 1970) and (Skillings, 1987). Attempt was also made by (Guha, 1990) to model the supercritical heat addition effect by using Denton's method (Denton, 1983). The method adopts the unsteady time-marching treatment for condensing flow of steam. However, the frequency was over-predicted and ranges from 540 Hz to 650 Hz. In recent decades, the study of supercritical heat addition in high speed condensing flow was also made by (White & Young, 1993) and (Yusoff et al., 2003). The predicted frequency was calculated to be 420 Hz and 393 Hz respectively.

In this work, the modified 1D model has been applied to calculate the effect of unsteady supercritical heat addition in Skilling nozzle (Skillings, 1987). The calculation is carried out in an unsteady mode until the solution converged into a steady oscillation. Fig. 13 illustrates the effect of supercritical heat addition to the static pressure in the nozzle. To investigate the unsteady effect accurately, the variations of static pressure at a point located just downstream of the nozzle's throat is plotted. In this case, higher oscillation was observed at the beginning of the iterations and the pressure variation settles at approximately 400 iterations. From this point, regular oscillation with a frequency of approximately 302 Hz is calculated. The inside figure illustrates the static pressure after stable and consistent oscillation is achieved. The pressure distribution is plotted against time for the calculation of the frequency. Tab. 2 shows the summary of frequencies calculated based on different authors using different numerical treatment. The prediction made by the current work shows reasonably good agreement as compared to the experimental data based on the Skillings nozzle.

Author	Case	Frequency, Hz	Pressure Difference, mbar
Skillings (1987)	Experiment	380	20
Skillings (1987)	1D program	640	-
Guha (1990)	1D program	540	-
White and Young (1993)	2D program	420	-
Yusoff et al. (2003)	2D program	393	18
Hasini et al. (2011)	1D program	302	17

Table 2. Frequency and pressure difference comparisons by different authors.

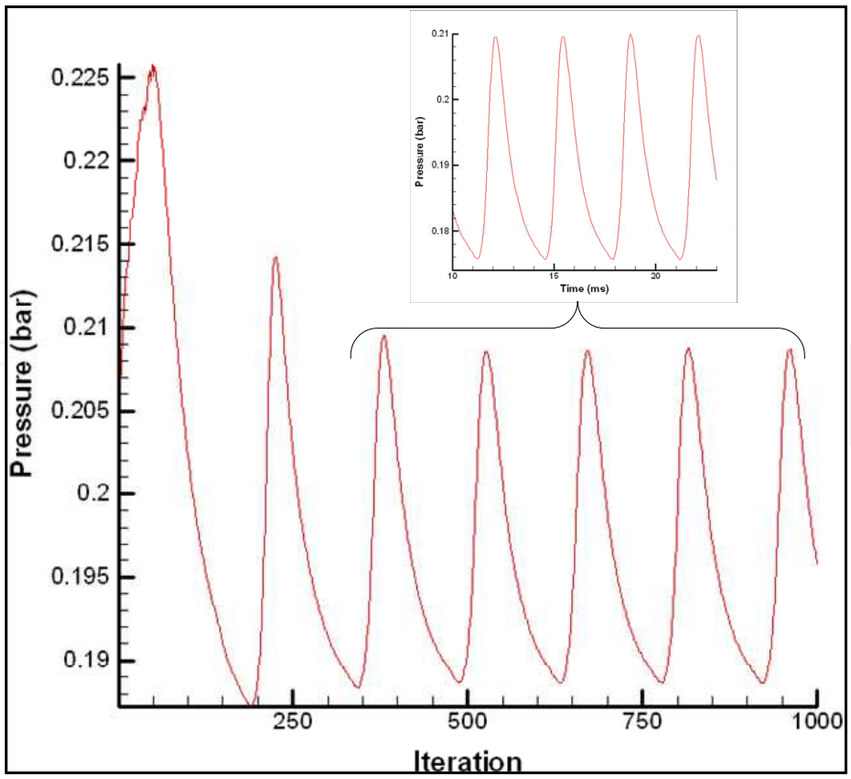

Fig. 13. Unstable supercritical heat addition effect to static pressure.

4.4 Polydispersed droplet calculations

Thus far, the calculation of droplet properties was averaged when a new droplet group formed with respect to time and space. This is done to simplify the calculation steps thus, reducing the computation time. In reality however, these droplet groups should be treated individually as their contribution to the total wetness inside the channel can be different. However, the calculation of the individual droplet spectrum is very complex and requires large computation power epecially when three-dimensional condensing flow is involved. Despite the simplications made in the calculation algorithm for the droplet properties, very little understanding was made on the effect of the calculation method in predicting the droplet properties. Thus this section aims to investigate the properties of wet steam given by individual droplet group tracking (called Non-Averaged method) and the average droplet property (called the Averaged method). The polydispersed droplet calculation is carried out where different droplet group formation and growth is tracked individually. In this study, the effect of droplet property averaging is carefully compared and investigated.

Fig. 14 shows the progressive growth of individual droplet group as superheated steam enters a constant area duct at 1 bar and initially at 44.8K supercooled. In order to observe their individual behavior, the droplets formed during each incremental step of the calculation have been regarded as a distinct group and treated separately. It can be seen that the variations in the critical droplet size, r^* is unaffected at the beginning but increases as the fluid become less supercooled. To investigate the behavior of the droplets, the variation of the radii of each individual droplet group is plotted separately. Taking droplet group (1) as

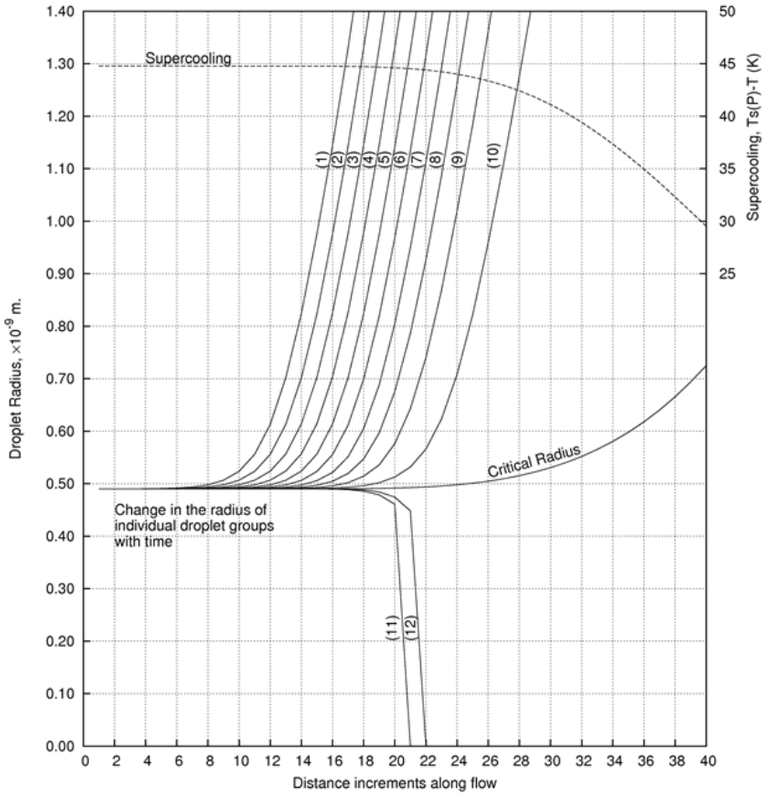

Fig. 14. Development of the early stage of nucleation (The numbers on curves refer to specific droplet groups).

an example, it will be seen that the rate of growth of this droplet group is initially small but rises rapidly as soon as they grow beyond critical radius. The pattern is similar for the next 9 droplet groups but a different behavior is observed in the case of groups (11) and (12). With the depletion of the supercooling, the critical radius increases. The newly formed droplet embryos in group (11) has a radius which is less than the critical radius. Consequently, this droplet group is unable to grow and survive (due to its initial radius which is less than the critical radius) and therefore, it will evaporate. This is represented by the sudden drop in radius as in Fig. 15. Thus, with the step size adopted in the calculation, the nucleation process can be assumed to be effectively over after the formation of droplet group (10). By selecting a shorter step size, the number of droplet groups will increase but the number of droplets in each group will fall, increasing both the accuracy and the volume of algebra to be calculated. In this work, the step length was adjusted to keep the number of droplet groups to approximately 10.

After the nucleation phase, the droplet groups are combined into a single population and their properties are averaged. For the example given in this work, the changes in relevant fluid properties after the nucleation phase are given in Fig. 15. It can be seen that, as expected, after the nucleation stage, the droplets grow rapidly at the beginning but with the depletion of supercooling, the rate of growth reduced and becomes extremely slow as the fluid approaches thermodynamic equilibrium. Similar profile can be seen for the wetness fraction where rapid increase in wetness is predicted at the beginning but as supercooling reduced, the rate at which water forms also reduced.

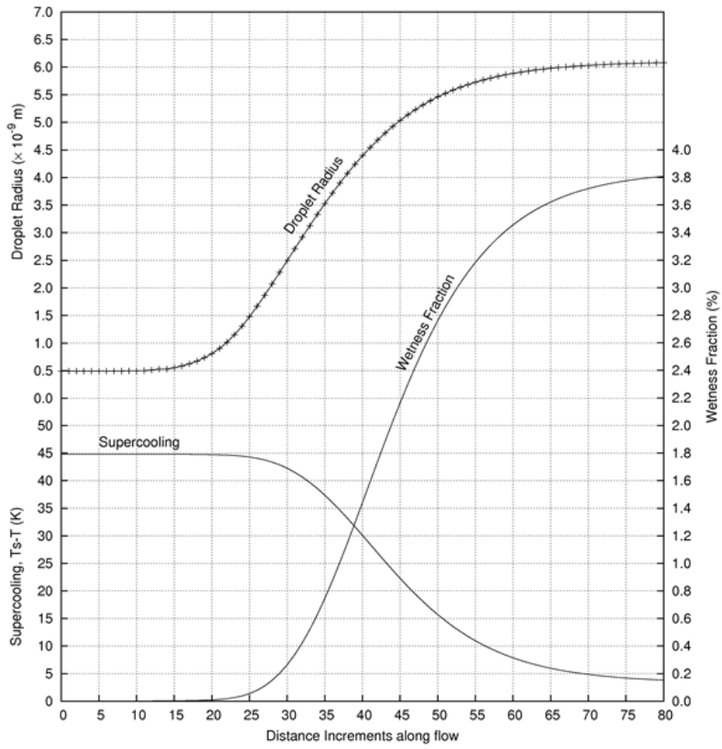

Fig. 15. Change in fluid properties during the return to equilibrium.

In order to check for the accuracy between the calculation procedures in estimating fluid properties after the completion of nucleation phase, comparison is made between the

"Averaged" and "Non-Average" methods. The comparison of the changes in the relevant fluid properties between the "Average" and "Non-Average" methods is shown in Fig. 16. In general, the supercooling and wetness fraction show similar trend for both methods. However, the average method seems to under-predict the droplet radius after the nucleation phase. This is probably due to the simplifications made to the governing equations and calculation procedure when numerical sensor created in the scheme automatically ignores the subsequent droplet embryos which grows for a very short period of time and later failed to survive. The cumulative error resulting from this simplification seems to increase at a very slow pace and later becomes constant. The maximum magnitude of this error is estimated to be approximately 5%. Taking into account the wetness fraction and supercooling properties predicted by both methods, and considering the amount of resources required by the Non-average method, it is anticipated that the Average method is capable of estimating the fluid properties in condensing flow. With some minor modification towards the numerical scheme, the scheme can be adopted to the real steam turbine passage for the prediction of various fluid properties in wet steam flow.

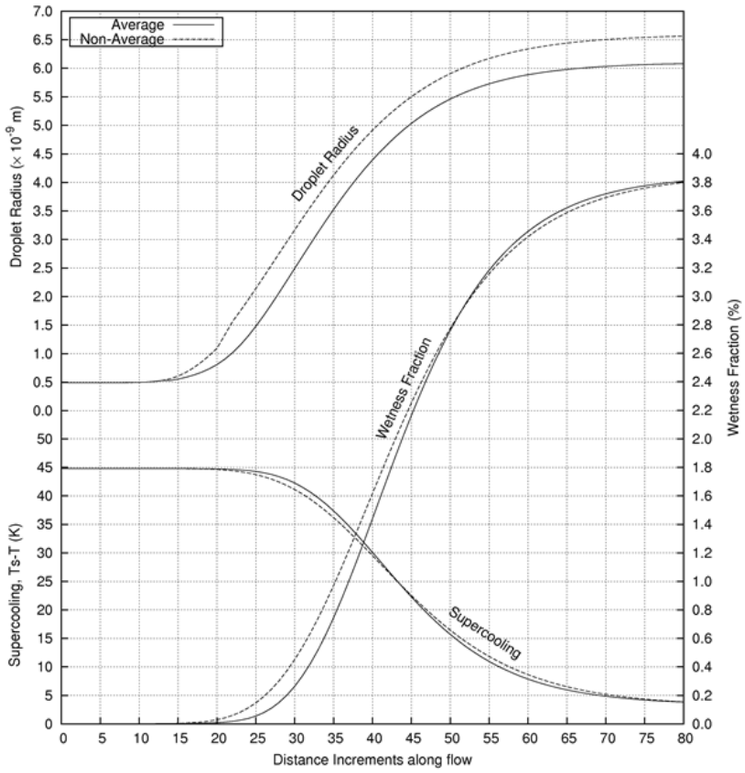

Fig. 16. Comparison on the changes of fluid properties between the "Average" and "Non-Average" methods.

5. Conclusion

The mathematical model for the calculation of high speed condensing flow has been developed. This model was applied to different test cases involving dry and wet flow expansion in converging-diverging nozzle. The mathematical prediction shows excellent agreement with experimental data for pressure along the nozzle. However, the calculated

droplet size in a few test cases only shows reasonable agreement with the measure size. The case for unsteady supercritical heat addition also reveals promising results indicating the capability of the model to calculate this phenomenon which might cause instability in turbine channel. The polydispersed droplet calculation has also been carried out using the model. Two methods of calculation were tested and compared. The first method tracks the individual droplet groups at the beginning of nucleation process. Upon the completion of nucleation, the droplet groups are combined into a single population and its properties are averaged. The "averaged" properties are repeatedly used for the subsequent steps until equilibrium. The second method however, retains the calculation of individual droplet groups and their properties and is called the "Non-Average" method. Comparison between the two methods reveals similar trend and even though the average methods slightly under-predicts the droplet radius after the completion of nucleation, the method is thought to be more suitable and economical due to considerable saving in computation time and processing power as compared to the other method. In addition, it is also anticipated that the discrepancies between the two methods are relatively small and therefore can be regarded as negligible.

6. References

Aitken, J. (1881). On Dusts, Fogs and Clouds. *Trans. Royal Society (Edinburgh)*, Vol. 30, pp.337-368

Barschdorff, D. (1970). Droplet Formation, Influence of Shock Waves and Instationary Flow Patterns on Condensation Phenomena at Supersonic Speed, *Proc. 3rd Intl. Conf. on Rain Erision and Allied Phenomena*, Farnborough

Becker, R. & Doring, W. (1935). Kinetische Behandlung der Keimbildung in Ubersettigten Dampfen. *Ann. D. Phys.* (Leipzig), Vol. 24, pp. 719-752

Binnie, A.M. & Wood, M.W. (1938). The Pressure Distribution in a Convergent-Divergent Steam Nozzle. Proc. Instn. Mech. Engrs, Vol. 138, pp. 229-226

Binnie, A.M. & Greem, J.R. (1943). An Electrical Detertor of Condensation in High-Velocity Steam. *Proc. Royal Society (London), A*, Vol. 181, pp. 134-154

Callender, H.L. (1915). On the Steady Flow of Steam Through a Nozzle or Throttle, *Proc. Instn. Mech. Engrs.*, pp. 53-77

Campbell, B.A. & Bakhtar, F. (1970). Condensation Phenomena in High Speed Flow of Steam. *Proc. Instn. Mech. Engrs.*, Vol. 185, pp. 395-404

Deich, M.E.; Tsiklauri, G.V.; Shanin, V.K. & Danilin, V.S. (1972). Investigation of Flows of Wet Steam inNozzles. *Teplofizika Vysokikh Temperatur*, Vol. 1, Part. 1, pp. 122-129

Denton, J.D. (1983). An Improved Time-Marching Method for Turbomachinery Flow Calculation. *ASME Paper 82-GT-239*

Farkas, L. (1927). Keimbildungsgeschwindigketit in Ubersettingten Dampfen, *Z. Phys. Chem.*, Vol. 125, pp. 236-242

Filippov, G.A. & Povarov, O.A. (1980). Moisture Separation in the Turbines of Nuclear Power Station. *Energy*, Moscow, pp. 329

Frenkel, J. (1946). *Kinetics Theory of Liquid*. Oxford University Press, London

Gerber, A.G. & Mousavi, A. (2007). Application of Quadrature Method of Moments to the Polydispersed Droplet Spectrum in Transonic Steam Flows with Primary and Secondary Nucleation. *Applied Mathematical Modelling*, Vol. 31, pp. 1518-1533

Guha, A. (1990). The Fluid Mechanics of Two-Phase Vapour Droplet Flow with Application to Steam Turbine, *Ph.D Thesis*, University of Cambridge, UK

Gyarmathy, G. (1962). Grundlagen einer Theorie der Nassdampfturbine. *Dissertation ETH, Zurich, Juris-Verlag* (English Translation: CEGB (London) Rept T-781 (1963))

Gyarmathy, G. & Meyer, H. (1965). Spontane Kondensation. *VDI Forschungsheft 508*, VDI-Verlag, Dusseldorf

Henderson, J.B. (1913). Theory and Experiment in the Flow of Steam Through Nozzle, *Proc. Instn. Mech. Engrs.*, Part 1, Vol. 2, pp. 253-314

Hill, P.G. (1966). Condensation of Water Vapour During Supersonic Expansion in Nozzles. *J. Fluid Mech.,* Vol. 25, Part 3, pp. 593-620

Krol, T. (1971). Results of Optical Measurement of Diameters of Drops Formed due to Condensation of Steam in a Laval Nozzle. *Trans. Instn. Fluid Flow Machinery (Poland)*, Vol. 57, pp. 19-30

Martin, H.M. (1918). A New Theory of the Steam Turbine, *Engineering*, Vol. 106, pp. 1-3, 53-55, 107-108, 161-162, 189-191, 245-246

Nikkhahi, B.; Shams, M. & Ziabasharhagh, M. (2009). A Numerical Investigation of Two-Phase Steam Flow Around a 2D Turbine's Rotor Tip. *Int. Comm. Heat and Mass Transfer*, Vol. 36, pp.632-639

Oswatitcsh, K.L. (1942). Condensation Phenomena in Supersonic Nozzle. *Z. Angew. Math. Mech.,* Vol. 22, Part 1, pp. 1-14 (RTP Translation no. 1905)

Pouring, A.A. (1965). Thermal Choking and Condensation in Nozzle, *Physics of Fluids*, Vol. 8, Part 10, pp. 1802-1810

Puzyrewski, R. (1969). Condensation of Water Vapour in a Laval Nozzle. *Instn. Fluid Flow Machinery*, Gdansk (Poland)

Rettaliata, J.T. (1938). Undercooling in Steam Nozzle. *Transaction of ASME*, Vol. 58, pp. 599-605

Skilling, S.A. (1987). An Analysis of the Condensation Phenomena Occuring in Wet Steam turbine, *Ph.D Thesis*, University of Birmingham, UK

Stodola, A. (1915). Undercooling of Steam Through Nozzle. *Engineering*, pp.643-646

Volmer, M. & Weber, A. (1996). Keimbildung in Ubersettingten Gebilden, *Z. Phys. Chem.*, Vol. 119, pp. 227-301

Von Helmholtz (1886). Untersuchungen über Dämpfe und Nebal, Besonders über Solche von Losungen. *Ann. D. Phys.*, Vol. 27. Pp. 508

Wegener, P.P. (1969). Gas Dynamics of Expansion Flows with Condensation and Homogeneous Nucleation of Water Vapour. *Non-Equilibrium Flows* (P.P. Wegener ed.), Marcel-Dekker, New York, Vol. 1, pp. 163-243

Wilson, W.T.R. (1897). Condensation of Water Vapour in the Presence of Dust-free Air and Other Gases. *Phil. Trans. Royal Society (London) A*, Vol. 189, pp. 265-307

White, A.J. & Young, J.B. (1993). Time Marching Method for the Prediction of Two-Dimensional Unsteady Flow of Condensing Steam, J. Propulsion and Power, Vol. 9, No. 4

Wroblewski, W.; Dykas, S. & Gepert, A. (2009). Steam Condensing Flow Modeling in Turbine Channels. *Int. J. Multiphase Flow*, Vol. 35, pp. 498-506

Yellot, J.L. (1934). Supersaturated Steam. *Transaction of ASME*, Vol. 56, pp. 411-430

Yellot, J.L & Holland, C.K. (1937). The Condensation of Flowing Steam, Part 1 – Condensation in Diverging Nozzles. *Transaction of ASME,* Vol. 59, pp. 171-183

Yusoff, M.Z.; Hussein, I.; Boosroh, M.H.; El-Awad, M.M. & Ahmad, Z. Numerical Simulation of Unsteady Flow Due to Supercritical Heat Addition during Condensation, *Advanced Technology Congress*, 2003.

Zeldovich, J. (1942). Theory of Nucleation and Condensation. Soviet *Physics – JETP (English Translation)*, Vol. 12, pp. 525

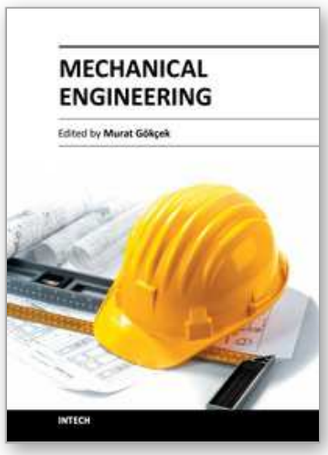

Mechanical Engineering

Edited by Dr. Murat Gokcek

ISBN 978-953-51-0505-3
Hard cover, 670 pages
Publisher InTech
Published online 11, April, 2012
Published in print edition April, 2012

The book substantially offers the latest progresses about the important topics of the "Mechanical Engineering" to readers. It includes twenty-eight excellent studies prepared using state-of-art methodologies by professional researchers from different countries. The sections in the book comprise of the following titles: power transmission system, manufacturing processes and system analysis, thermo-fluid systems, simulations and computer applications, and new approaches in mechanical engineering education and organization systems.

InTech Europe
University Campus STeP Ri
Slavka Krautzeka 83/A
51000 Rijeka, Croatia
Phone: +385 (51) 770 447
Fax: +385 (51) 686 166
www.intechopen.com

InTech China
Unit 405, Office Block, Hotel Equatorial Shanghai
No.65, Yan An Road (West), Shanghai, 200040, China
中国上海市延安西路65号上海国际贵都大饭店办公楼405单元
Phone: +86-21-62489820
Fax: +86-21-62489821

IntechOpen